PCCP

Cite this: *Phys. Chem. Chem. Phys.*, 2011, **13**, 10848–10857

www.rsc.org/pccp

PERSPECTIVE

Adventures in ozoneland: down the rabbit-hole†

Neil M. Donahue,*[a] Greg T. Drozd,[a] Scott A. Epstein,[a] Albert A. Presto[a] and Jesse H. Kroll[b]

Received 16th November 2010, Accepted 25th February 2011
DOI: 10.1039/c0cp02564j

In this perspective we describe a 15 year pursuit of the Stabilized Criegee Intermediate (SCI). We have conducted several complementary experiments to measure the pressure dependence of product yields—including OH radical and ozonides—on sequences of alkene + ozone systems. In so doing we have been able to bring into gradual focus a succession of weakly bound intermediates, starting with the primary ozonide, then the SCI, and finally a vinyl hydroperoxide (VHP) product of SCI rearrangement. We have narrowed the phase space in our hunt for direct SCI observations to a range of alkene carbon numbers and system pressures, but the system continues to deliver surprises. One surprise is strong evidence that the VHP is a significant bottleneck along the reaction coordinate. These findings support the search for the SCI, build our fundamental understanding of collisional energy transfer in highly excited, multiple-well, chemically activated systems, and finally directly inform atmospheric chemistry on topics including HO_x radical formation and reactions associated with secondary organic aerosol formation.

1. Introduction

We have been pursuing ozonolysis intermediates for fifteen years. This is a small portion of our story pertaining to three wells along one branch of the ozonolysis potential energy surface (PES). Things are getting curiouser and curiouser.

Gas-phase ozonolysis is extremely exothermic, and the PES following the initial 1,3-dipolar cycloaddition of ozone to the alkene double bond is riddled with shallow wells, low barriers, and multiple branch points. Ozonolysis initiates the oxidation of many unsaturated organic compounds emitted into Earth's atmosphere, most notably terpenoid compounds emitted copiously from vegetation.[1,2] Alkene ozonolysis can be an important source of radicals (notably OH), initiating further oxidation in the troposphere.[3] The terpenes are very important sources of secondary organic aerosol (SOA),[4,5] and SOA yields depend on reaction mechanisms because SOA formation requires production of very low vapor-pressure reaction products.[6]

In the gas phase, collisional energy transfer is the only way for ozonolysis products to lose excess energy, and so they will remain chemically activated for many nanoseconds. The lifetimes of the excited, weakly bound intermediates are often much shorter than the collisional frequency, and so the system can explore a significant amount of territory on the PES before thermalization. However, those unimolecular lifetimes are also strong functions of the number of atoms (and thus the number of internal degrees of freedom) of the product molecules. Consequently, the dynamics can show a strong pressure dependence, and homologous sequences can show a strong dependence on carbon number.

In this article we shall focus on a small subset of the weakly bound intermediates along one pathway of especially important ozonolysis products—the carbonyl-oxides, or Criegee Intermediates (CI) in a syn configuration. Criegee Intermediates were first proposed by Rudolph Criegee[7] as crucial players in ozonolysis, and their carbonyl oxide structure was confirmed by a combination of mechanistic evidence[8] and computational chemistry.[9] However, clear isolation of stabilized Criegee Intermediates (SCI) remains a major objective, and despite tantalizing evidence from a less energetic source,[10] the SCI remains elusive. Our objective is to track down the SCI, but here we shall reveal only shadows on the wall while identifying some of the properties that contribute to its elusiveness.

2. Background

A canonical PES for the portion of the reaction coordinate we shall discuss is shown in Fig. 1 for the reaction of cyclohexene with ozone.[11] The key features are the large exothermicity and the succession of weakly bound intermediates. The first

[a] *Center for Atmospheric Particle Studies, Carnegie Mellon University, Pittsburgh, USA. E-mail: nmd@andrew.cmu.edu; Fax: +01 412 268 7139; Tel: +01 412 268 4415*
[b] *Departments of Civil and Environmental Engineering and Chemical Engineering, MIT, Boston, USA*

† This article was submitted as part of a collection following the 21st International Symposium on Gas Kinetics, held in Leuven in July 2010.

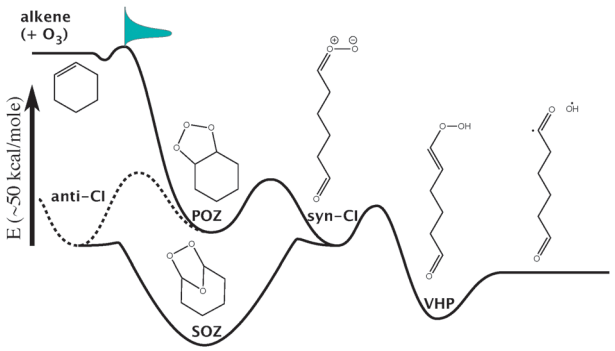

Fig. 1 Partial potential energy surface for the cyclohexene + ozone reaction. Energies are approximate, with the arrow indicating roughly 50 kcal/mole. Formation of the primary ozonide (POZ) is sharply exothermic, with a low cycloreversion barrier leading to carbonyl-oxides, or Criegee Intermediates (CI). This PES focuses on the syn conformer of the CI (syn-CI); a second conformer, the anti-CI, can also form—a small portion of this PES is shown with a dashed line. The syn-CI can isomerize to form a vinyl hydroperoxide (VHP), which can then decompose along the O–O bond, yielding OH radicals and an organic radical. Alternatively, the CI can react with a carbonyl (in this case the terminal moiety of the same molecule) to form a secondary ozonide (SOZ). The initial reaction energy is indicated by the Boltzmann distribution on the cycloaddition transition state.

intermediate is the primary ozonide (POZ), or 1,2,3-trioxolane intermediate. The second intermediate is the CI, which is formed in conjunction with a carbonyl co-product (CCP). The co-product is a separate, stable molecule for linear alkenes but for endocyclic alkenes such as the cyclohexene shown in Fig. 1 it exists as a distal moiety on the CI. The CI can lead to a secondary ozonide (SOZ), or 1,2,4-trioxolane, which is the typical product in classical ozonolysis discussed for liquid-phase synthetic applications.[12] For linear alkenes, the SOZ forms from the bimolecular recombination of the CI with the CCP, while for endocyclic alkenes the SOZ can form *via* re-cyclization of the CI containing both functional groups.[11] However, in the gas phase, isomerization of the CI to either a vinyl hydroperoxide (VHP), as shown here,[9] or a dioxirane[13] is thought to predominate. Whether the VHP or dioxirane is formed appears to depend heavily on the conformation of the CI—specifically whether the terminal oxygen faces an alkyl group (Syn-CI) or a hydrogen (Anti-CI), as shown:

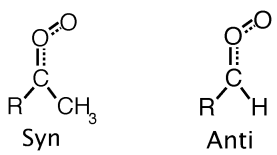

The Syn–CI favors the VHP because the H-atom abstraction transition state has lower ring strain than it does for the Anti-CI, and also because formation of the double bond in the VHP requires the adjacent carbon atoms present in that configuration.[14,15]

The other crucial issue concerning the unimolecular dynamics is the energy distribution and unimolecular lifetimes of the intermediates. The unimolecular lifetime depends on both the fractional excess energy over the lowest reaction barrier as well as the molecular size (number of internal modes, s). In the simplest RRK terms:

$$k(E)_{\mathrm{RRK}} = \nu\left(\frac{E - E_0}{E}\right)^{(s-1)} \qquad (1)$$

This competes with the frequency at which the excited molecule collides with the bath gas (ω), generally about 10^{10} Hz at 1 bar pressure. Our detailed master equation calculations for substituted cyclohexenes show that adding 5 carbons is roughly equivalent to increasing the pressure (ω) by about 1 order of magnitude at the very high excess energies shown in Fig. 1.[11]

As long as there is a single reaction product, the pre-collision (nascent) energy distribution of an intermediate will be narrow and large, as indicated by the Boltzmann distribution in Fig. 1. Once the molecule breaks into fragments (if it does), the energy is distributed among the fragments in a quasi-statistical manner, with a residual going into external degrees of freedom (translation and external rotation). However, the details of the energy distribution upon fragmentation are quite uncertain.[16] Two things occur simultaneously: the excess energy ($E - E_0$ in eqn (1)) in the fragment is reduced (potentially by a substantial amount), but the fragment size (*i.e.*, s in eqn (1)) declines as well. Consequently, the overall effect on stabilization is complex. However, there is one critical difference between the single-product and fragmented situation: as long as there is only a single product, we expect the energy to be quite narrowly distributed, but once the products fragment, each can have a broad distribution of internal energies. In fact, some may be formed with too little energy to decay ($E < E_0$); what fraction that is "born cold" upon decomposition is one of the many questions we have sought to answer. We thus expect qualitatively different behavior from endocyclic and linear alkenes ("linear" meaning a double bond without a bridging functional group).

3. Three wells full of tears or treacle

We have explored ozonolysis along the PES shown in Fig. 1 using a number of experimental techniques, augmented by quantum-chemical calculations and statistical reaction dynamics (multi-well master equation simulations). In this discussion we shall move smoothly from left to right along the reaction coordinate, though historically we have jumped around the PES less systematically. Also, we have selected a few alkenes for special attention: 2,3-dimethyl-2-butene (tetramethylethylene, or TME), several centrally unsaturated *n*-alkenes (*i.e.* 2-butene, 5-decene, *etc.*), cyclohexene and some substituted analogues, and finally α-pinene as a canonical endocyclic monoterpene associated with secondary organic aerosol (SOA) formation.[4] These alkenes allow us to explore the effects of increasing carbon number, substitution, and the different behavior of endocyclic *vs.* linear alkenes.

3.1 Primary ozonide

The first significant intermediate on the PES is the POZ. With extreme excess energy and a large unimolecular pre-exponential factor, the chemically activated POZ decomposes readily. Our calculations suggest that a carbon number between 15 and 20

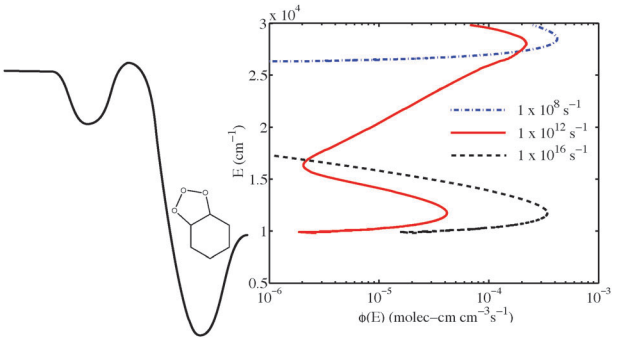

Fig. 2 Calculated decomposition fluxes *vs.* energy (in cm^{-1}) for the cyclohexene POZ for different collisional frequencies (ω, s^{-1}), which are proportional to pressure. At low pressure (dot-dashed blue curve at top) the energy distribution of the flux is unaltered from the formation flux—there has been no stabilization and consequently the system shows extreme, narrowly distributed chemical activation. One atmosphere is approximately 10^{10} Hz, so the red curve shows the beginning of some (a few percent) stabilization at 100 bar pressure. By 1 megabar pressure (well above even condensed-phase collision frequencies and thus an unphysical situation), the POZ is completely stabilized and the thermal decomposition flux (dashed black curve at bottom) dominates. Calculations suggest that increasing the carbon number (n_C) by 5 is roughly equivalent to a 1-decade increase in ω; thus, an alkene with $n_C \simeq 16$ has a POZ decomposition flux at 1 bar similar to the red curve.

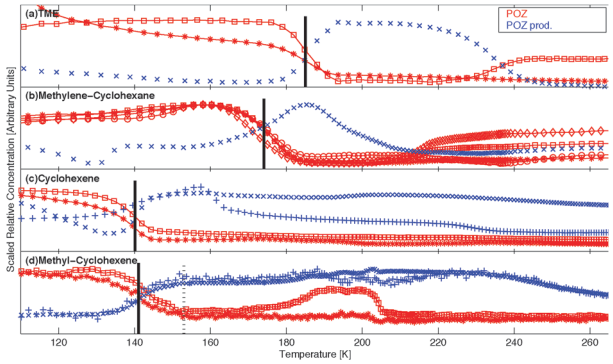

Fig. 3 Temperature programmed reaction spectra for ozonolysis of (a) TME, (b) methylene-cyclohexene, (c) cyclohexene, and (d) methyl-cyclohexene. IR features associated with the POZ are shown in red with a connecting curve, while features associated with reaction productes are shown in blue as symbols only. For TME, the spectrum of the product is consistent with the secondary ozonide (SOZ). The POZ decomposition temperature (T_D) is defined as the inflection point on the sigmoidal POZ intensity curve. In each panel T_D is identified with a vertical solid line. A second value of T_D at 155 K in panel (d) identified with a dotted line shows where a second, higher energy barrier would be seen if it were visible; it is not. For the linear or exocyclic alkenes (a) and (b), T_D is near 180 K, while for the endocyclic alkenes (c) and (d) it is near 140 K. This shows that the cycloreversion barrier is significantly lower in these later cases.

is necessary for substantial stabilization of the POZ at atmospheric pressure[11] (this should hold regardless of the alkene, as the essential POZ structure remains constant through the full sequence of reactions). In Fig. 2 we show calculated decomposition fluxes ($\Phi(E)$) *vs.* energy at several collisional frequencies (pressures). The conclusion is that below C_{15} the majority of the flux to the subsequent well (the CI) will have essentially full chemical activation (the dashed blue curve).

Because stabilization of the POZ in the gas phase is difficult, we elected to study the POZ by depositing ozone and an alkene on a cryogenically cooled IR-transparent window, following the method first described by Heicklen and co-workers[17] but largely ignored afterwards. By carefully mounting a small ZnSe window on the end of a cold finger exactly in the waist of a focused IR beam, we were able to isolate the POZ from a sequence of alkenes and then perform temperature programmed reaction spectroscopy (TPRS) by tracking key features with real-time FTIR.[18] Fig. 3 shows results for TME, methylene-cyclohexene (an analogue of β-pinene), cyclohexene, and methyl-cyclohexene. The peak desorption temperatures (T_D) are indicated in each panel of Fig. 3, and a straightforward Redhead analysis allows us to relate T_D in each case to the cycloreversion barriers.[18,19]

There are two key findings from this work. First, the endocyclic alkenes have systematically lower cycloreversion barriers (9–9.5 kcal/mole) than the exocyclic or linear alkenes (12–14 kcal/mole). The effects of cyclization appear to dominate over the effects of substitution in this regard (though our sample size is small). Second, there is no sign of an additional decomposition step (or product formation) for any of the asymmetric systems (b–d). The product spectra are also consistent with a single, dominant product.[19] This indicates that the reaction is very selective at these low temperatures.

The selectivity of the cycloreversion is directly relevant to the relative formation probability of syn and anti-CI. According to density-functional theory calculations, the next lowest of the four cycloreversion barriers from methyl-cyclohexene is almost 2 kcal/mole higher than the lowest-energy barrier.[19] The corresponding value of T_D is shown in Fig. 3(d), and it is evident that POZ has completely decomposed before this critical temperature is reached. The cycloreversion selectivity is thus controlled principally by energetic factors (as opposed to entropic factors in the cycloreversion pre-exponential term). This difference in barrier heights does suggest that POZ stabilization will differ for endocyclic and linear alkenes, but all of the measured barriers are somewhat lower than the 16.5 kcal/mole cyclohexene POZ barrier used in our earlier computational study.[11] In that work we found roughly 10% POZ stabilization for a carbon number of 15 at 1 atmosphere. Recent work on β-caryophyllene (a C_{15} sesquiterpene) suggests that the 1 atm stabilization may be 65%,[20] but these values are quite consistent giving the uncertainties in unimolecular reaction dynamics (*i.e.* ΔE_{down}).

3.2 Carbonyl-oxide (Criegee Intermediate)

The second well on our reaction coordinate is the Criegee Intermediate. Formation of the SCI is of special interest as it has been put forward as a potentially important reactive species in atmospheric chemistry;[21–23] however, to be important, SCI must first be formed. For the endocyclic alkenes, the nascent CI should still retain most of the initial reaction energy, while for the linear and exocyclic alkenes the CI should be formed with a wide range of energies. Theory thus indicates that SCI formation should make a fairly sharp transition from essentially zero to a large value at some (generally large)

pressure for endocyclic alkenes; the pressure falloff curve should resemble a Lindemann-Hinshelwood form because the nascent CI will all have similar unimolecular lifetimes. Contrarywise, for linear alkenes SCI formation should rise steadily from some finite value at zero pressure (indicating the fraction of CI "born cold") and progressing toward unity. The falloff curve should be very broad because of a wide distribution of nascent CI unimolecular lifetimes, and the center of the falloff curve should move toward lower pressure with increasing carbon number.

We have carried out studies of SCI formation using two scavengers: hexafluroacetone (HFA) and NO_2. The scavenger experiments were carried out using reaction modulation spectroscopy[24] in two high-pressure flow systems. The salient features of these experiments are that the stable reagents are mixed with carrier gas (N_2) in a wide (12–20 cm) flowtube, while reactive compounds (ozone in this case) are added *via* a sidearm injector to the center of the tube, leading to a reactive plume in the center of the tube that remains isolated from the tube walls for the duration of the experiment. The reaction is monitored *via* FTIR using a transverse multi-pass White cell, and the chemistry is modulated by turning the reactive gas flow on and off repeatedly, leading to a difference spectrum in which reagent consumption and product formation across the plume can be measured directly. With scavenger experiments, sufficient scavenger is added to completely titrate the reactive intermediates, generally very quickly, and the resulting stable scavenging products float downstream to the White cell in a few seconds. This is an advantage over direct measurements because even short-lived intermediates can be scavenged on a short chemical timescale but observed over longer timescales (and thus using much less carrier gas).

3.2.1 Hexafluroacetone scavinging. The HFA experiments are the most recent and the most direct. HFA reacts selectively with SCI to form a secondary ozonide (HFA-SOZ) that is easy to identify.[25] The only available reactive site on HFA is the carbonyl (a dipolarophile), and that is very selective toward a 1-3 dipolar cycloaddition with the carbonyl-oxide 1-3 dipole.

We have recently explored the pressure dependence of HFA-SOZ production for four alkenes—TME, trans-5-decene, cyclohexene, and α-pinene.[26,27] The results are summarized in Fig. 4. We observe a broad pressure dependence for the linear alkenes, with TME below the center of its falloff curve ($Y_{SCI} < 0.5$) for most of the pressure range and trans-5-decene above the center of the falloff curve for the full range. TME also clearly shows an intercept at zero pressure, indicating that about 15% of the CI (acetone–oxide) is formed with insufficient internal energy to decompose at the low-pressure limit. On the other hand, trans-5-decene reaches an asymptotic

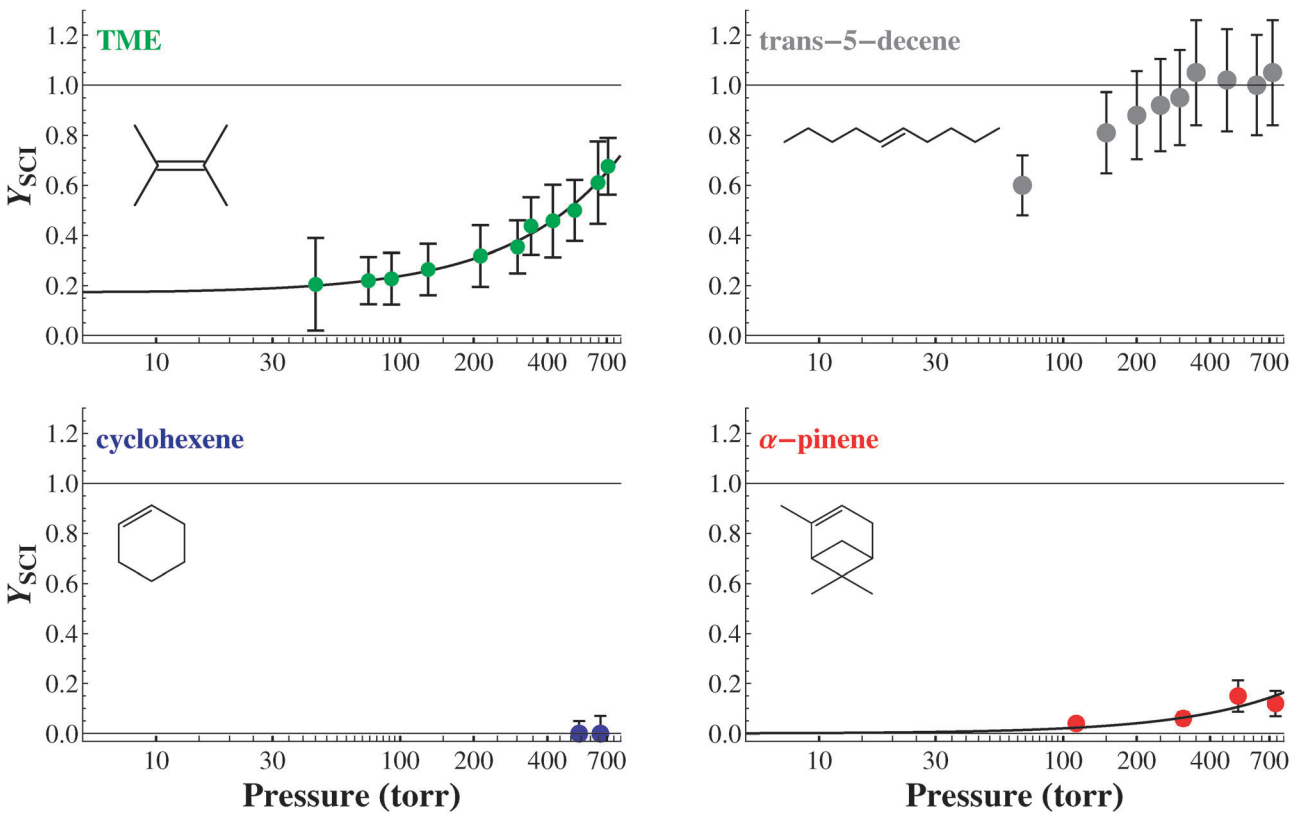

Fig. 4 Stabilized Criegee Intermediate formation *vs.* pressure for a sequence of alkenes, measured by titration with hexafluroacetone (HFA) to form a secondary ozonide. The linear alkenes TME and trans-5-decene show a strong pressure dependence. For TME the SCI yield is about 15% at the low-pressure limit, indicating that this fraction is formed with internal energy below the decomposition threshold. The center of the falloff curve is at roughly 1 bar (760 torr). For trans-5-decene the center of the falloff curve is lower by an order of magnitude, and SCI formation is complete by about 400 torr. Endocyclic alkenes show almost no SCI formation; none at all is observed for cyclohexene, while roughly 15% is formed from α-pinene at 760 torr.

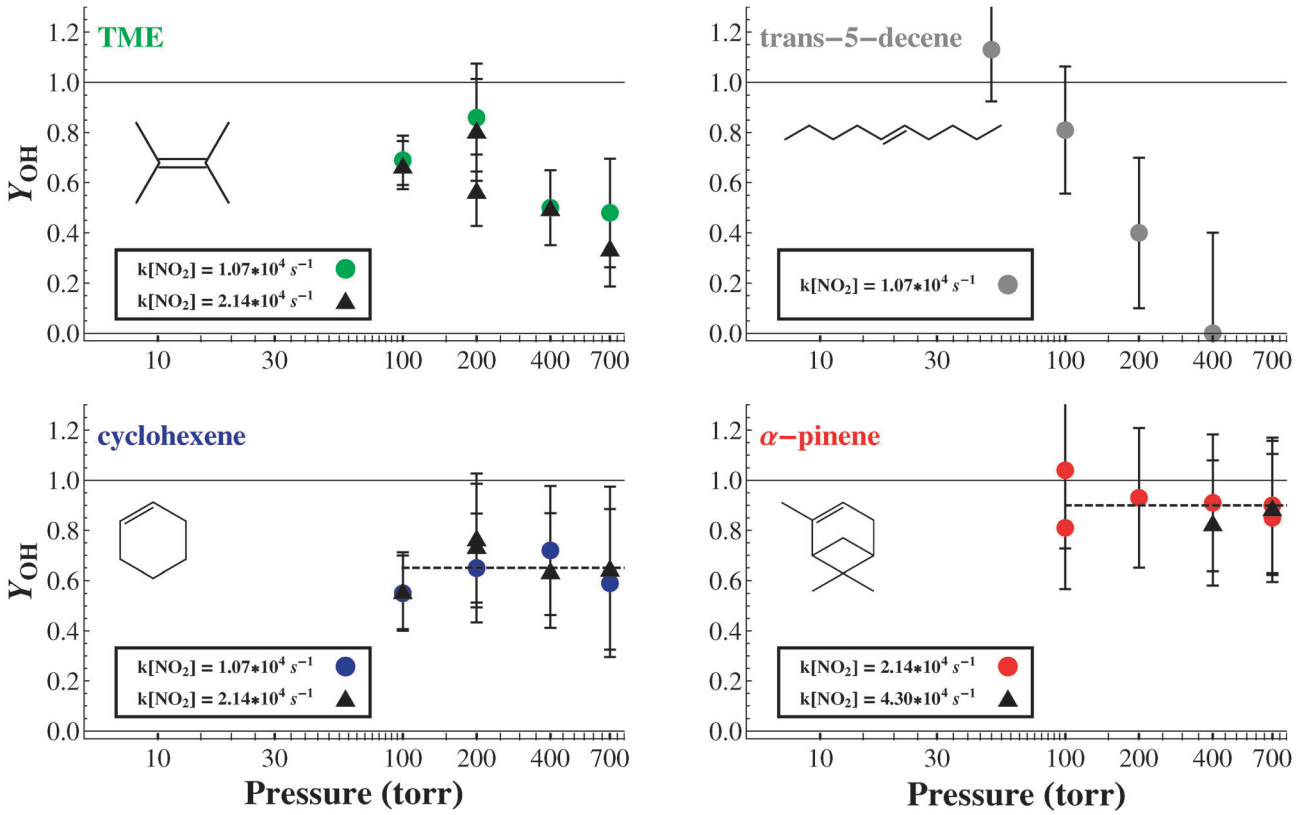

Fig. 5 OH yields based on NO_2 scavenging *vs.* pressure for a sequence of alkenes. Some correction must be applied for the OH + NO_2 reaction; the rate of this reaction was held constant at two different values to test the correction, with good agreement as shown. OH yields are roughly the inverse of the SCI yields shown in Fig. 4 based on HFA scavenging. TME shows a strong pressure dependence with the center of the falloff curve near 760 torr while trans-5-decene shows a strong pressure dependence at roughly a factor of 10 lower pressure. Neither cycloalkene shows any significant pressure dependence; the absolute OH yields reflect the syn-anti selectivity of these two systems.

high-pressure limit consistent with 100% SCI formation at approximately 400 torr. Together, the linear alkene data are consistent with 3–4 added carbons shifting the pressure dependence by roughly 1 decade. The ''shift'' per carbon is larger than with POZ stabilization because at lower energy the system is more sensitive to the number of modes (the carbon number) and less sensitive to the pre-exponential factor, which should be roughly constant with increasing carbon number.

The cycloalkene data are dramatically different, again as anticipated. Cyclohexene shows no evidence whatsoever of SCI formation. In fact, this was a strong test of our theoretical predictions. α-Pinene, however, does show a small but statistically significant yield of SCI at 1 atm pressure of approximately 15%, which declines with reduced pressure consistent with zero yield at the zero-pressure limit. Both cycloalkenes are thus deep in the low-pressure limiting regime where we expect SCI yields to be well below unity and to increase linearly with increasing pressure.

One additional finding is that the α-pinene SCI is evidently long-lived enough to permit a reaction with HFA, thus disproving our theoretical finding of rapid self-conversion to an SOZ through a reaction of the carbonyl–oxide and carbonyl moieties of the single reaction product.[11] This pathway is certainly on the PES (as indicated in Fig. 1), but the critical issue is the barrier height for the cyclization reaction—a barrier of even a few kcal/mole may be sufficient to permit bimolecular scavenging by HFA. Other studies have found evidence for the anti-SCI in this system reverting to the SOZ,[28] as shown in the dashed portion of Fig. 1; our results do not directly confirm or refute those findings.

As a whole, the HFA scavenger experiments are consistent with our theoretical expectations—linear alkenes show evidence that the nascent CI products span a wide range of internal energies, and that a 5-carbon CI can be quite readily stabilized well below 1 atm pressure. Endocyclic alkenes, however, clearly behave like compounds with uniformly high internal energy, and despite the much larger carbon numbers for the intermediates (and thus much lower intrinsic RRKM rate constants at a given energy) only begin to hint at stabilization with the 10-carbon precursor.

3.2.2 NO_2 scavenging. A second useful scavenger is NO_2. The difference between NO_2 and HFA is that NO_2 is anything but selective. Instead, it reacts with essentially any compound containing radical or 1–3 dipole character, including ozone and carbonyl oxides, but also including all of the radical fragments arising from further decomposition chemistry. Most notably, NO_2 will react with OH to form nitric acid, and NO_2 will react with the SCI to form both NO_3 and the carbonyl co-product (essentially in a reductive workup).[29] Because of this, we can use measured OH yields (in the form of nitric acid) to partially constrain the yield of *unstabilized* Criegee

Intermediates ($1 - Y_{SCI}$). This is only a partial constraint because the measurement also depends on the yield of OH radicals from unstabilized Criegee Intermediates. The evidence points to a yield of approximately 1.0 for syn-CI (*via* the hydroperoxide pathway shown in Fig. 1[30]) and approximately 0.15 for the hot acid formed from anti-CI.[31] Furthermore, H-atom production (from the hot acid) will also appear as nitric acid, as the reaction H + NO_2 → OH + NO is very rapid. We technically measure OH + H, but there are no gross disagreements with more direct OH measurements, suggesting that H-atom formation is a minor pathway for these systems.

Using this as a probe of unstabilized CI, we will miss approximately 85% of any unstabilized anti-CI. We shall assume that any pressure dependence in the observed OH formation is due to CI stabilization (mostly syn-CI stabilization), as the resulting SCI would be scavenged by NO_2 and thus not decompose to make any OH—this assumption is verified by both quantum chemical calculations as well as observed increases in acetone formation with pressure in NO_2 scavenging experiments.[29]

The results of our NO_2 scavenging experiments are shown in Fig. 5. As described in the original paper,[29] the data analysis involves some treatment of the multiple reaction pathways of NO_2, and we performed experiments at several different NO_2 concentrations to ensure that we were not sensitive to complex NO_2 (and OH) chemistry, holding the (pressure dependent) value of $k(NO_2+OH) \times [NO_2]$ constant at two different values in most cases. In general, doubling the amount of NO_2 did not change the OH yields, which showed that the intermediates had been completely scavenged.

Fig. 5 is an exact parallel to Fig. 4, except the yields are anti-correlated: as the SCI yields increase, the OH yields decrease. However, the figures show qualitative and quantitative agreement in almost all regards. First, the TME system reaches about 60% stabilization and 40% (prompt) OH production at 760 torr (1 atm) pressure. Second, trans-5-decene reaches a high-pressure limit of 100% stabilization and no prompt OH at about 400 torr. Finally, neither of the endocyclic alkenes show any sign of a significant pressure dependence; the OH yield is not unity because both cyclohexene and α-pinene do form some anti-CI products. Many independent studies have shown that the anti-CI yields (at 300 K) from cyclohexene are near 40% and from α-pinene are near 20%[28,32–35] The small amount of stabilization we observe for α-pinene at 760 torr *via* HFA scavenging is well within the noise of the OH yields in Fig. 5.

In summary, both sets of scavenger experiments confirm that the linear alkenes show substantial collisional stabilization, but that the endocyclic alkenes (up to C_{10}) show almost none. The data are consistent with each other and consistent with theoretical calculations. Direct observation of the SCI would be greatly simplified by complete stabilization at or below about 100 torr pressure, as that could in principle lead to a very simple product distribution with manageable flow conditions in a flow reactor. This goal can be met by using 6-dodecene or 7-tetradecene as the reagent alkene.

3.3 OH formation *via* vinyl hydroperoxides

Time runs oddly down the rabbit-hole, and so it does in our story. Our interest in ozonolysis began in the mid 1990s with an emerging controversy about whether radical yields based on scavenger consumption[36–38] were indeed indicative of OH production or perhaps some other unidentified radical species.[39] To address this issue we decided to employ direct detection of OH *via* Laser Induced Fluorescence (LIF) in the Harvard High-Pressure Flow (HPF) kinetics system,[40,41] exploiting the fact that any OH produced from an ozone + alkene reaction would be immediately consumed by the alkene, resulting in a straightforward steady-state expression for the OH yield α_{OH}:

$$\alpha_{OH} = \frac{k_{OH}[OH]}{k_{O_3}[O_3]} \quad \text{or} \quad \alpha_{OH} = \frac{k_{OH}}{k_{O_3}}\frac{\partial[OH]}{\partial[O_3]} \qquad (2)$$

The differential form is preferable as it reduces experimental errors.[42] The obvious challenge with this approach is that it requires accurate absolute measurements of the OH radical, which is not trivial.

3.3.1 Pressure-dependent OH LIF. However, even without perfectly accurate OH measurements, the pressure dependence of OH production can be explored (even then one must account for quenching of the OH LIF signal). To solve the calibration challenge, we adapted the Harvard-HO_x LIF instrument to explore OH yields from ozonolysis.[43] The instrument was designed for stratospheric OH and HO_2 measurement covering the relevant pressure range.[44] This allowed us to cross-calibrate the precise but less accurate LIF measurements in the HPF kinetics flow system (where precision but not LIF accuracy is the principal experimental requirement).

Fig. 6 shows the OH yields from the the TME + ozone reaction measured with both the Harvard HO_x instrument (large black circles)[43] and the HPF LIF instrument[45] as a function of pressure. As with the scavenger experiments, there is a clear decrease in the OH yield with increasing pressure. Even the zero-pressure intercept of the OH yield (about 15%) is in near perfect agreement with the 15% SCI formation observed at low pressure using the HFA scavenger. We do not have LIF yield data for the exact sequence of reagents shown in Fig. 4 and 5, but the LIF data also consistently reveal a pressure dependence that gets progressively stronger (stabilization at lower pressures) with increasing carbon number for linear alkenes.[43,45]

In spite of the general agreement for the TME data, there is a substantial difference in the pressure dependence derived from the direct OH measurements and from the scavengers. The scavenger measurements both indicate that only about half of the TME CI (acetone oxide) has stabilized at 760 torr, and yet the LIF data in Fig. 6 reach 50% stabilization below 50 torr. This is summarized in Fig. 7. There is more than one order of magnitude separation in the critical pressure for stabilization observed *via* direct LIF measurement and *via* scavengers, and both observations are confirmed by multiple measurements. Consequently, there is compelling evidence that the observed differences have a root cause in the reaction itself and not a systematic difference in the experiments.

3.4 Multiple wells, multiple effects

One of the reasons that TME is such an appealing reagent to anchor these studies is its high symmetry; another is its high reactivity towards ozone, which results in good signal to noise

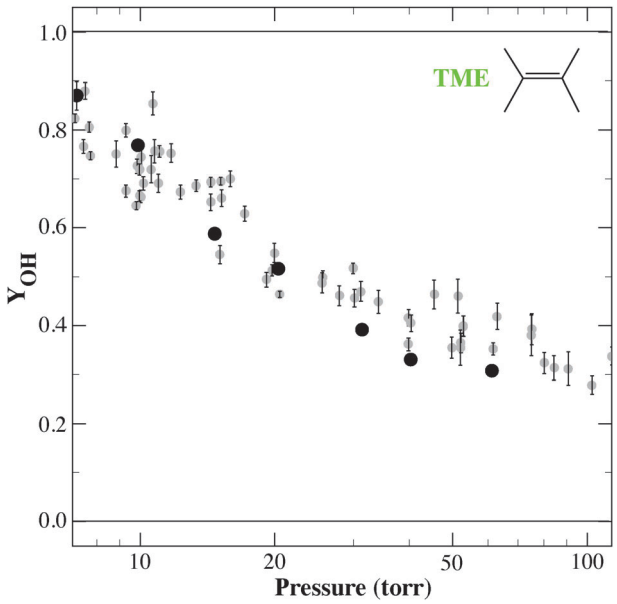

Fig. 6 OH production from the TME + ozone reaction as a function of pressure, measured directly with two different LIF instruments approximately 10 ms downstream of the reaction initiation point. Highly accurate (±10%) measurements with the Harvard-HO_x *in situ* instrument are the dark black circles, while measurements with the Harvard high-pressure flow kinetics system are smaller gray symbols with error bars.

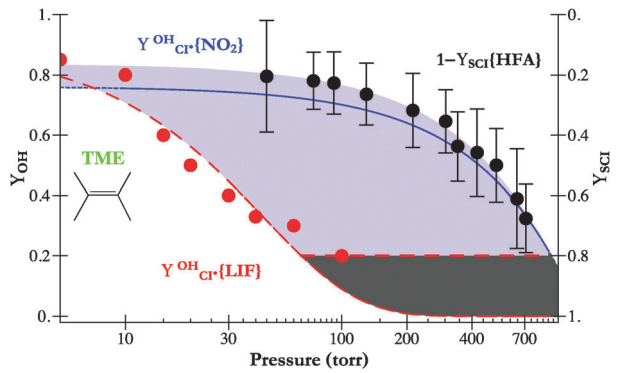

Fig. 7 Pressure stabilization of TME + ozone reaction products based on different measurements. LIF data (plain red circles and dashed red curve) show a rapid drop in OH production with pressure, while experiments employing SCI scavengers, including OH formation deduced from NO_2 scavenging (dotted blue curve) and the residual from the HFA SOZ yield experiments ($1 - Y_{SCI}$), black points with error) fall off a more than 1 order of magnitude higher pressure. All have a consistent low-pressure limit of ~80% prompt OH. The difference (gray shaded area) is most probably due to interception of the normal reaction sequence by the scavengers.

for our experiments. Because we expect only acetone and acetone–oxide (100% syn *via* symmetry) as reaction products, the system is confined entirely to the relatively simple syn-CI reaction coordinate shown in Fig. 1. Thus, any pressure dependence should be a result of stabilization into one of the wells along the solid curve in the figure. As we have already discussed, there is no reason to believe that any stabilization occurs into the POZ well (and the cyclohexene scavenger data confirm this). Consequently, the stabilization should be into either of the SCI or the vinyl hydroperoxide (VHP) wells. Neither of these wells is very deep, so we would expect even those stabilized products to decompose thermally in short order. This is precisely what we have observed,[15] as shown in Fig. 8. In the HPF system (without any scavengers) the OH signal that was lost to pressure quenching at short reaction times (of order 10 msec) returns in 300–500 msec.

We previously interpreted the LIF pressure and time dependence as being indicative of stabilization into and decomposition out of a single intermediate well—the SCI.[15] This was partly to simplify the modeling, but also because it has been commonly assumed that the VHP decomposition does not retard the progress of the reaction because it is assumed to be a barrierless bond scission[11,45,46] well below the SCI decomposition energy, as shown in Fig. 1. We now have reason to doubt that assumption.

The straightforward explanation for the difference in pressure falloff curves shown in Fig. 7 is that the LIF measurements are sensitive to stabilization in *either* the SCI or the VHP well while the scavenger measurements (because they scavenge SCI) are sensitive only to stabilization in the SCI well (technically, any well before or including the SCI). In this explanation, the gray region in Fig. 7 corresponds to stabilization into the VHP well where there was little or no stabilization into the SCI, while the region below the LIF data (dashed curve) corresponds to a true crawl along the minimum PES, with stabilization first into the SCI followed by a second stabilization into the VHP before any thermal decomposition to OH and other products.

Under this interpretation, the time dependence in Fig. 8 would be due to VHP thermal decomposition, and with a

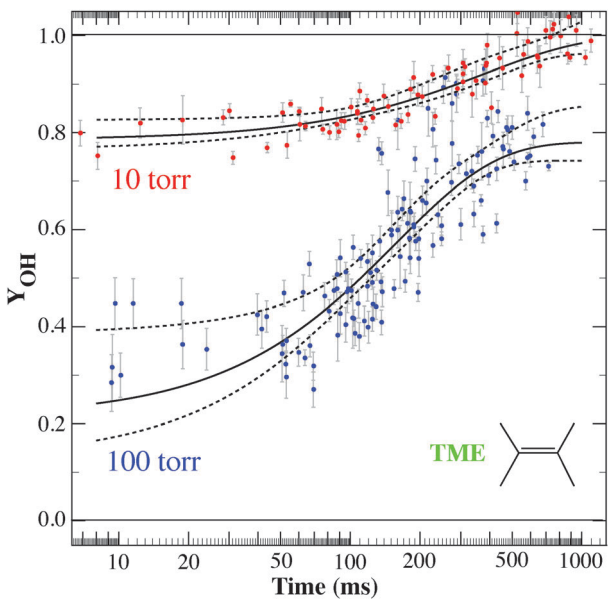

Fig. 8 Time dependence of the TME + ozone OH LIF signal at two pressures. Most or all of the pressure dependence in the OH LIF signals occurs only at times less than 200 ms or so. This confirms that the pressure effect is due to stabilization into very weakly bound intermediates, which can thermally decompose in 200–300 ms.

theoretical bond energy of about 19 kcal/mole this is not beyond the pale. However, for this mechanism to be viable the unimolecular rate constants ($k(E)$) for VHP decomposition need to be below roughly 10^9 Hz at modestly high energies, which is not consistent with a simple scission. The answer may lie in the time dependence of the VHP decomposition. The lowest-energy form of the organic radical product is the keto-alkyl radical shown on the right-hand side of the scheme below. However, the O–O bond cleavage correlates diabatically with the vinoxy configuration shown to the left. If the reconfiguration leads to even a small barrier, or alternatively a time delay, it is possible that there could be a sufficient holdup for energetically excited compounds over the VHP well to be collisionally stabilized at 100 torr pressure, consistent with our data.

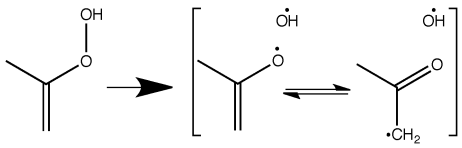

We therefore hypothesize that most of the pressure effect observed for prompt OH formation *via* LIF is due to collisional stabilization into the VHP well, rather than the CI. That is why we have presented the OH LIF results in the VHP section.

4. Elsewhere in the garden

We have so far confined our discussion almost entirely to a single pathway along the complex ozonolysis PES—the syn-CI mediated production of OH. However, our research over the years has strayed considerably from this simple path.

4.1 anti-CI

The chemistry of Criegee Intermediates with the terminal oxygen facing a hydrogen atom rather than an R group—anti-CI—is dramatically different from syn-CI. This difference is a key indication that the CI contains substantial zwitterionic character, as without it the barrier to syn-anti interconversion would be very low, and consequently the syn-CI and anti-CI chemistries would be identical or nearly so.

Whereas the lowest free energy pathway for the syn-CI is the VHP channel we have discussed, it is thought that the anti-CI undergoes a ring closure to a dioxirane, followed by a distinct ring opening to a bis-oxy radical (this step contains a conical intersection on the O–C–O angle and bond distance coordinates). The bis-oxy radical immediately forms a "hot acid" (formic acid in the canonical ozone + ethene system), which was originally hypothesized to be the major intermediate for OH production.[13]

However, decomposition of the hot acid is complex, with many open channels. Ozone + ethene has a low (15%) OH yield,[13,43,47] but the OH yield from other anti-CI systems is uncertain. By synthesizing selectively deuterated cis- and trans-3-hexene with deuteriums adjacent to the double bond, Kroll *et al.*[31] were able to show that the anti-CI produced from 3-hexene ozonolysis also produces OH (or OD) with a roughly 15% yield, suggesting that anti-CI in general produce OH radicals with about 15% yield.

4.2 Secondary organic aerosol

Aerosol formation from ozonolysis is a major source of SOA,[4,5] and in addition to extensive studies of the SOA yields from ozonolysis reactions, we have studied the ozonolysis mechanism to help provide fundamental mechanistic detail for the yield measurements. In particular, we have been able to show that the more substituted carbonyl oxide is heavily favored when the exo double bond is oxidized by ozone by synthesizing limonaketone (which would be the co-product if formaldehyde–oxide were formed) and comparing SOA yields from limonaketone to limonene itself.[48] The substantially

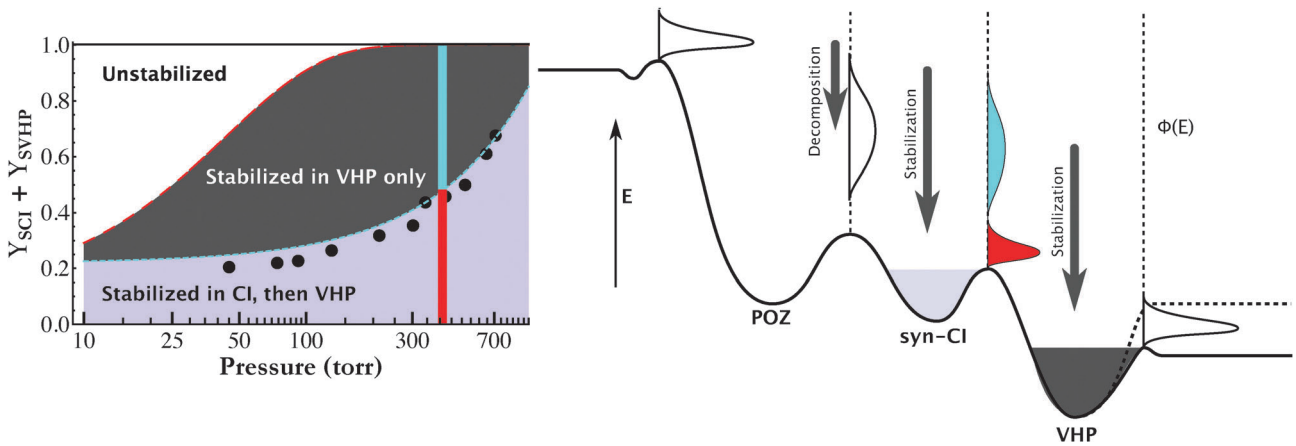

Fig. 9 Hypothesized behavior along the syn-CI reaction coordinate. The left-hand panel shows stabilization fractions *vs.* pressure for TME + O_3 constrained by direct OH LIF (upper curve) and Criegee Intermediate scavengers (middle curve and data points). Interpretation on the PES is in the right-hand panel for 400 torr (indicated by vertical bars in the left-hand panel), where stabilization is about 50% for SCI scavengers and 100% for OH LIF. Curves at each transition state (indicated with vertical dashed lines) are reactive fluxes. Essentially no stabilization occurs in the POZ well, but when the POZ decomposes the CI is formed with a broad energy distribution. Half of the molecules are stabilized into the syn-CI well (light gray region in the left-hand panel and the syn-CI well), so the shaded output flux from the syn-CI well is bimodal. All of the molecules are stabilized into the VHP well (dark gray), including the thermally decomposing SCI (lower mode) and the chemically activated CI (upper mode), so the output flux from the VHP (at 400 torr) is completely thermal.

higher SOA yields for limonene confirm that functionalized products following the exo ozonolysis (from the equivalent of the limonaketone–oxide) are responsible for the much higher SOA yields observed for the doubly unsaturated limonene compared with singly unsaturated monoterpenes such as α-pinene.[49,50]

A more general question concerns what happens after the VHP decomposes. Canonical gas-phase hydrocarbon chemistry would suggest that, under low-NO_x conditions, a highly substituted β-keto hydroperoxide would be formed after some rapid radical-radical reactions involving the keto-alkyl radical shown above.[36] We have conducted two-dimensional heteronuclear NMR (HSQC) analyses of filter extracts from limonene + O_3 to explore this possibility, and indeed the resulting spectra show a rich collection of features with both H- and ^{13}C shifts consistent with those structures.[51]

5. Conclusions and future directions

At the end of the rabbit-hole lies testable speculation, which is summarized in Fig. 9 for TME + O_3 at about 400 torr. While even "simple" SOA formation systems have many reaction prodcts, for the first few hundred ms the chemistry may be fairly simple, at least for molecules that can be stabilized. Stabilization is the key. We have tantalizing evidence that we can achieve complete stabilization at 100 torr pressure of SCI compounds starting from C_{12}–C_{14} precursors, but these SCI will probably only live for a few hundred ms (at most) before decomposing. Our data on POZ decomposition confirm that the cycloreversion barrier is so low that almost no POZ will be stabilized below C_{15}, even at 760 torr. After SCI stabilization the intermediate may drop into another well, the VHP, where even C_8 or C_{10} precursors may be completely stabilized at 100 torr. Those intermediates too appear to live for only a fraction of a second.

To isolate the ozonolysis SCI cleanly, we must drop the molecule into the second of the three wells in Fig. 9 and keep it there for a sufficiently long time to observe it. It seems to be fairly simple to avoid falling into the POZ well, but landing in (and staying in) the SCI well may be trickier. However, the separation may be possible. Our goal is to form SCI with 100% yields at 100 torr simply because of the large carrier gas flow required to keep the FTIR White cell within 100 ms of the ozone injection point in our flowtube. This may be a recipe for conclusive observations of the elusive Criegee Intermediate, white kid gloves and all.

References

1 J. P. Greenberg, A. Guenther, P. Harley, L. Otter, E. M. Veenendaal, C. N. Hewitt, A. E. James and S. M. Owen, *J. Geophys. Res.*, 2003, **108**, 8466.
2 A. Goldstein and I. Galbally, *Environ. Sci. Technol.*, 2007, **41**, 1515–1520.
3 S. Paulson and J. Orlando, *Geophys. Res. Lett.*, 1996, **23**, 3727.
4 J. H. Kroll and J. H. Seinfeld, *Atmos. Environ.*, 2008, **42**, 3593–3624.
5 M. Hallquist, J. C. Wenger, U. Baltensperger, Y. Rudich, D. Simpson, M. Claeys, J. Dommen, N. M. Donahue, C. George, A. H. Goldstein, J. F. Hamilton, H. Herrmann, T. Hoffmann, Y. Iinuma, M. Jang, M. E. Jenkin, J. L. Jimenez, A. Kiendler-Scharr, W. Maenhaut, G. McFiggans, T. F. Mentel, A. Monod, A. S. H. Prévôt, J. H. Seinfeld, J. D. Surratt, R. Szmigielski and J. Wildt, *Atmos. Chem. Phys.*, 2009, **9**, 5155–5236.
6 J. Odum, T. Hoffmann, F. Bowman, D. Collins, R. Flagan and J. Seinfeld, *Environ. Sci. Technol.*, 1996, **30**, 2580.
7 R. Criegee, *Rec. Chem. Proc.*, 1957, **90**, 414.
8 P. S. Bailey, N. L. Bauld, J. A. Thompson and C. E. Hudson, *J. Am. Chem. Soc.*, 1968, **90**, 1822.
9 D. Cremer, *J. Am. Chem. Soc.*, 1981, **103**, 103.
10 C. A. Taatjes, G. Meloni, T. M. Selby, A. J. Trevitt, D. L. Soborn, C. J. Percival and D. E. Shallcross, *J. Am. Chem. Soc.*, 2008, **130**, 11883–11885.
11 B. Chuong, J. Zhang and N. M. Donahue, *J. Am. Chem. Soc.*, 2004, **126**, 12363–12373.
12 P. S. Bailey, *Ozonation in Organic Chemistry, vol. I*, Academic Press, 111 Fifth Ave., New York, NY, 10003, 1978.
13 J. Herron and R. Huie, *J. Am. Chem. Soc.*, 1977, **99**, 5430.
14 D. Cremer, *J. Chem. Phys.*, 1979, **70**, 1911.
15 J. H. Kroll, S. Shahai, J. Anderson, K. L. Demerjian and N. Donahue, *J. Phys. Chem. A*, 2001, **105**, 4446–4457.
16 M. J. Pilling and P. W. Seakins, *Reaction Kinetics*, Oxford University Press, Oxford, 1996.
17 J. Heicklen, I. C. Hisatsune and L. A. Hull, *J. Am. Chem. Soc.*, 1972, **94**, 4856.
18 S. A. Epstein and N. M. Donahue, *J. Phys. Chem. A*, 2008, **112**, 13535–13541.
19 S. A. Epstein and N. M. Donahue, *J. Phys. Chem. A*, 2010, **114**, 7509–7515.
20 T. L. Nguyen, R. Winterhalter, G. Moortgat, B. Kanawati, J. Peeters and L. Vereecken, *Phys. Chem. Chem. Phys.*, 2009, **11**, 4173–4183.
21 A. S. Hasson, G. Orzechowska and S. E. Paulson, *J. Geophys. Res.*, 2001, **106**, 34131.
22 A. S. Hasson, A. W. Ho, K. T. Kuwata and S. E. Paulson, *J. Geophys. Res.*, 2001, **106**, 34143.
23 B. Bonn, A. Hirsikko, H. Hakola, T. Kurtén, L. Laakso, M. Boy, M. Dal Maso, J. M. Mäkelä and M. Kulmala, *Atmos. Chem. Phys.*, 2007, **7**, 2893–2916.
24 N. M. Donahue, K. L. Demerjian and J. G. Anderson, *J. Phys. Chem.*, 1996, **100**, 17855–17861.
25 O. Horie, C. Schäfer and G. K. Moortgat, *Int. J. Chem. Kinet.*, 1999, **31**, 261–269.
26 G. T. Drozd, J. H. Kroll and N. M. Donahue, *J. Phys. Chem. A*, 2011, **115**, 161–166.
27 G. T. Drozd and N. M. Donahue, *J. Phys. Chem. A*, submitted.
28 R. Atkinson, S. M. Aschmann, J. Arey and J. Tuazon, *J. Phys. Chem. A*, 2003, **107**, 2247.
29 A. A. Presto and N. M. Donahue, *J. Phys. Chem. A*, 2004, **108**, 9096–9104.
30 R. Gutbrod, R. N. Schindler, E. Kraka and D. Cremer, *Chem. Phys. Lett.*, 1996, **252**, 221.
31 J. H. Kroll, V. J. Cee, N. M. Donahue, K. L. Demerjian and J. G. Anderson, *J. Am. Chem. Soc.*, 2002, **124**, 8518–8519.
32 R. Atkinson, S. M. Aschmann, J. Arey and B. Shorees, *J. Geophys. Res.*, 1992, **97**, 1337.
33 R. Atkinson and S. M. Aschmann, *Environ. Sci. Technol.*, 1993, **27**, 1357.
34 S. Paulson, J. Fenske, K. Kuwata and K. N. Houk, *J. Phys. Chem. A*, 2000, **104**, 7246.
35 J. Calvert, R. Atkinson, J. Kerr, S. Madronich, G. Moortgat, T. Wallington and G. Yarwood, *The Mechanisms of Atmospheric Oxidation of the Alkenes*, Oxford University Press, 2000.
36 R. Atkinson, *Atmos. Environ.*, 1990, **24A**, 1.
37 G. Marston, C. D. McGill and A. R. Rickard, *Geophys. Res. Lett.*, 1998, **25**, 2177.
38 S. E. Paulson, J. D. Fenske, A. D. Sen and T. W. Callahan, *J. Phys. Chem. A*, 1999, **103**, 2050.
39 C. Schäfer, O. Horie, J. M. Crowley and G. K. Moortgat, *Geophys. Res. Lett.*, 1997, **24**, 1611.
40 J. P. D. Abbatt, K. L. Demerjian and J. G. Anderson, *J. Phys. Chem.*, 1990, **94**, 4566–4575.
41 N. M. Donahue, J. S. Clarke, K. L. Demerjian and J. G. Anderson, *J. Phys. Chem.*, 1996, **100**, 5821–5838.
42 N. M. Donahue, J. H. Kroll, J. G. Anderson and K. L. Demerjian, *Geophys. Res. Lett.*, 1998, **25**, 59–62.

43 J. H. Kroll, T. F. Hanisco, N. M. Donahue, J. G. Anderson and K. L. Demerjian, *Geophys. Res. Lett.*, 2001, **28**, 3863–3866.
44 P. O. Wennberg, R. C. Cohen, N. L. Hazen, L. B. Lapson, N. T. Allen, T. F. Hanisco, J. F. Oliver, N. W. Lanham, J. N. Demusz and J. G. Anderson, *Rev. Sci. Instrum.*, 1994, **65**, 1858–1876.
45 J. H. Kroll, J. S. Clarke, N. M. Donahue, J. G. Anderson and K. L. Demerjian, *J. Phys. Chem. A*, 2001, **105**, 1554–1560.
46 M. Olzmann, E. Kraka, D. Cremer, R. Gutbrod and S. Andersson, *J. Phys. Chem. A*, 1997, **101**, 9421–9429.
47 S. E. Paulson, M. Y. Chung and A. S. Hassan, *J. Phys. Chem. A*, 1999, **103**, 8125.
48 N. M. Donahue, J. E. Tischuk, B. J. Marquis and K. E. Huff Hartz, *Phys. Chem. Chem. Phys.*, 2007, **9**, 2991–2998.
49 J. Zhang, K. E. Huff Hartz, S. N. Pandis and N. M. Donahue, *J. Phys. Chem. A*, 2006, **110**, 11053–11063.
50 N. L. Ng, J. H. Kroll, M. D. Keywood, R. Bahreini, V. Varutbangkul, R. C. Flagan, J. H. Seinfeld, A. Lee and A. H. Goldstein, *Environ. Sci. Technol.*, 2006, **40**, 2283–2297.
51 C. S. Maksymiuk, C. Gayathri, R. R. Gil and N. M. Donahue, *Phys. Chem. Chem. Phys.*, 2009, **11**, 7810–7818.